Proc. of the Intl. Conf. on Advances In Civil, Structural And Construction Engineering - CSCE 2014.

ISBN: 978-1-63248-020-0 doi: 10.15224/ 978-1-63248-020-0-103

A CFD Study of a Naturally Ventilated Three-storey Simple Atrium Building

Shafqat Hussain, Nashmi H. Alrasheedi, S.M.F. Hasani, Patrick H. Oosthuizen

***Abstract*—The flow field and temperature distribution in a three-storey simple atrium building located in three different cities across Canada is numerically investigated at different times on a summer day. The building utilizes a buoyancy-driven natural ventilation system and has a curved glazed roof over the central portion. The numerical results are obtained using the commercial CFD solver ANSYS FLUENT©. The Reynolds Averaged Navier Stokes (RANS) equations are solved in conjunction with the SST-k-ω turbulence model and the Discrete Transfer Radiation Model (DTRM). Results for the ventilation air flow rate, the air pressure, the velocity, the turbulence intensity, and the temperature distribution inside the building at different times of the day are presented for the various locations considered in the study.**

***Keywords*—Building spaces, atria, turbulent natural convection with radiation, CFD analysis**

I. Introduction

External climatic conditions affect the architectural design of naturally ventilated buildings. The internal airflow pattern is the result of interaction between the indoor and outdoor environment. In particular, natural ventilation, and outdoor conditions strongly affect the indoor airflow pattern, and thus affect the thermal comfort of the occupants. The main purpose of natural ventilation is to draw as much of fresh and clean air as is required to bring the room temperature to a comfortable level. The open space concept of atria, with high ceilings, promotes temperature stratification, and hence enhances the thermal stack effect which helps in inducing the buoyancy-driven natural ventilation. The proper design of the natural ventilation systems must be based on the detailed understanding of airflow within enclosed spaces governed by pressure differences due to wind and buoyancy forces.

In recent years, Computational Fluid Dynamics (CFD) modeling has emerged as a useful tool to calculate airflow velocities and temperatures in indoor environments. It provides spatial information about velocities and temperature distributions in the flow field that allows evaluation of thermal comfort in the occupied areas of the buildings [1]. Modern building performance standards create a need for accurate and flexible simulation models that can contribute to a better design and increased use of low energy, naturally driven cooling systems. The ultimate aim of conditioning the interior environments of buildings is to provide a comfortable and healthy indoor environment for the occupants

Natural ventilation has been widely recognized as a means of reducing energy use in buildings. Conventional ventilation systems based on mechanical components consume electric power. Due to worldwide environmental concerns, the need to reduce energy use in buildings has increased the interest in natural ventilation strategies. Natural ventilation can be induced by wind flow over the building and by buoyancy forces induced by the temperature difference inside the building. In such cases, the stack pressure, which is the difference between the external and internal building pressure, is naturally created due to the density difference, and it drives the ventilation flow through the building. Architectural features that can enhance the stack effect, for example, tall solar chimneys, light wells and atria, have in recent times been increasingly employed. These structures potentially increase the height of the column of warm air inside the buildings and, as a result, increase the stack driving force drawing cooler air from the exterior – near the bottom or sides of the building – and venting it out after it has warmed by convective heat exchange with the internal space of the building. Advanced stack-ventilated atria buildings have the potential to consume less energy for space conditioning than typical mechanically ventilated buildings. The proper design of the natural ventilation system must be based on the detailed understanding of airflows within enclosed spaces governed by pressure differences due to wind and buoyancy forces. At the design stage, CFD modeling techniques can be utilized to investigate the ventilation flow rates, the temperature distribution and the thermal stratification within the ventilated space. [1-10].

Simple building geometries such as a single ventilated enclosure with openings connected to the exterior have been the subject of much research in order to gain a deeper understanding of the ventilation concepts. The key concern when devising these types of ventilation strategies is whether or not sufficient ventilation flow rates would be generated. The ultimate aim of conditioning the interior environments of buildings is to provide a comfortable and healthy indoor environment for the occupants. [11-13].

Ji et al. [14] studied the flow characteristics (thermal stratification and airflow rates) of buoyancy-driven ventilation in an atrium connected to single storey space by using a CFD model. The numerical results were compared with predictions

Shafqat Hussain, Nashmi H. Alrasheedi, S.M.F. Hasani
Al-Imam Mohammad Ibn Saud Islamic University, Riyadh
Saudi Arabia
shafqat55@yahoo.com

Patrick H. Oosthuizen
Queen's University, Kingston, Ontario
Canada
oosthuiz@me.queensu.ca

Proc. of the Intl. Conf. on Advances In Civil, Structural And Construction Engineering - CSCE 2014.

ISBN: 978-1-63248-020-0 doi: 10.15224/ 978-1-63248-020-0-103

of analytical models and small-scale experiments. They observed that the airflow patterns, temperature distribution and ventilation flow rates predicted by the CFD model agreed favorably with the analytical models and the experiments. Cook and Lomas [15] showed comparisons between analytical, experimental and CFD modeling of natural convection airflow in a single space with a localized point heat source and openings connected to the ambient environment. Allocca et al. [16] investigated the effect of single sided natural ventilation for rooms sharing a vertical ventilation space. A CFD model was used to assess the effects of buoyancy forces, wind and heat sources on the ventilation flow rates and the indoor conditions. Predicted results were compared with empirical and analytical solutions for the buoyancy-driven flow. The CFD results from their study were found to be within 10 percent of analytical solutions for buoyancy driven flow. Holford and Hunt [17] studied the flow field in a single ventilated space connected to a tall atrium and developed simple analytical models which they validated using small-scale salt bath experiments. They demonstrated that during the design stage the proposed techniques can be useful in understanding the flow characteristics, including the prediction of required ventilation flow rates, fresh air distribution and temperature distributions.

The purpose of the present study is to numerically investigate the buoyancy-driven natural ventilation airflow and temperature distribution induced by solar radiation and heat sources present on each floor of a multi-storey simple atrium building using a validated and tested CFD model, [7-10]. The model is developed using the commercial CFD simulation code ANSYS FLUENT©. This modeling effort is a part of a larger study exploring the application of natural ventilation for atria buildings in Canada. In the present study the performance of a simple three-storey atrium type building located in three different cities across Canada is numerically investigated at different times on a summer day.

The building utilizes a buoyancy-driven natural ventilation system and has a curved glazed roof over the central portion of the building. The Reynolds Averaged Navier Stokes (RANS) equations are solved using the SST- k-ω turbulence model and the Discrete Transfer Radiation Model (DTRM). It is assumed that at any particular time the flow is steady. Detailed analysis and results for ventilation airflow rates, pressure, velocity, turbulence intensity and temperature distributions inside the building are presented for the different geographical locations at various times of the day.

II. Building Description and Weather Data

The thermal environment in the atrium space of the Engineering Building of Concordia University, Montreal (lat. 45° 30' N; long. 73° 35' W) was previously studied by Hussain and Oosthuizen [9, 10] using a CFD model and the numerical results were validated against the available experimental data. Two more Canadian locations, Saint John (lat. 45°18' N; long. 66° 10' W) and Vancouver (lat. 49° 13' N; long. 123° 06' W) have been added in this study. The selected geometry of the simple atrium building shown in Figure 1 is similar to the one studied earlier [9, 10].

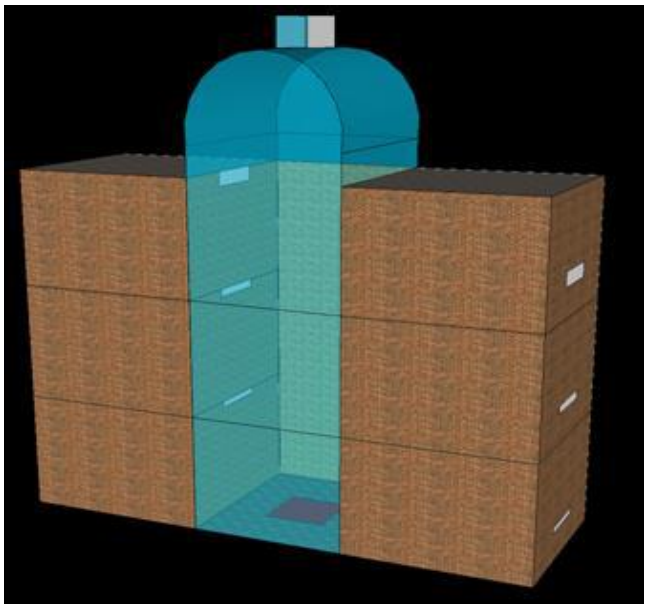

Figure 1. A simple three-storey atrium building with a curved glazed roof

The important dimensions and areas of the building are given in Table I. The orientation of all the three buildings is assumed same i.e. 35 degrees west of south, using similar type of glazing on the atrium roof and southwest facing facade. The atrium exhausts are located at the highest point in the atrium. Air supply inlets and outlets on each storey are located on the side walls of the rooms and atrium. The inlets and outlets on each storey are sized using the design curves developed by Holford and Hunt [17]. The effective atrium outlet opening area is selected to be equal to the total inlet opening areas for each storey.

TABLE I. AREAS AND DIMENSIONS OF THE ATRIUM BUILDING

Areas and Dimensions	
Atrium Height	16.00 m
Atrium Width	5.00 m
Atrium Depth	6.00 m
Room Height	4.00 m
Room Width	6.00 m
Room Depth	6.00 m
Façade Glass Area	80.00 m^2
Ground Floor air supply inlet (net) area	0.40 m^2
First Floor air supply inlet (net) area	0.54 m^2
second Floor air supply inlet (net) area	1.10 m^2
Atrium Floor air supply inlet area	0.20 m^2
Atrium outlet opening (net) area	2.14 m^2

The solar heat flux and ambient temperature values used in the simulations for the three locations are obtained from [18] and are given in Table II. The reason for choosing the 15th

Proc. of the Intl. Conf. on Advances In Civil, Structural And Construction Engineering - CSCE 2014.

ISBN: 978-1-63248-020-0 doi: 10.15224/ 978-1-63248-020-0-103

day

TABLE II. THE WEATHER DATA USED IN THE CFD SIMULATIONS

	Solar Heat Flux (W/m^2)			Ambient Temperature (^{o}C)		
15 July 2012	**9am**	**1pm**	**6pm**	**9am**	**1pm**	**6pm**
Saint John	1069.2	1205.0	766.1	18.2	25.0	23.0
Montreal	1018.3	1216.8	872.2	25.9	28.8	23.0
Vancouver	826.8	1180.1	941.0	15.5	17.1	18.5

of July for simulation is because Canada receives the maximum solar radiation in the month of July during summer and the average for the month is very closely approximated by the solar radiation received on the 15th day of July.

III. The Numerical Model

The airflow patterns and temperature distributions in the atrium building are governed by the conservation laws of mass, momentum and energy. The mathematical model applied includes the numerical techniques to solve the continuity, Navier-Stokes (*N-S*), and energy equations for incompressible, three-dimensional turbulent flow. The general form of the momentum, turbulent kinetic energy, turbulent energy dissipation, and energy (with constant heat capacity) equations in the steady-state form can be expressed in the general form as follows:

$$\frac{\partial(\rho u_i \varphi)}{\partial x_i} = \frac{\partial}{\partial x_i}(\Gamma_\varphi \frac{\partial \varphi}{\partial x_i}) + S_\varphi \qquad (1)$$

where variable (φ) represents (*u*), (*v*), (*w*), (*k*), (ε), (*T*) and (Γ_φ) is the diffusion coefficient of the variable (φ). S_φ represents the source terms including the pressure terms, thermal source terms, etc., as appropriate for the variable (φ) being solved. The solution involves the following assumptions: (i) single phase, steady-state flow of a Newtonian fluid (ii) the heat transfer through the walls is only by conduction and radiation is neglected for all walls except where glazing is used (iii) the atmospheric conditions are constant and (iv) the outside wind velocity is zero.

A. *Inputs and Boundary Conditions*

All boundaries of the domain, except the glazed façade surface, ventilation openings, and heat sources are modeled as no-slip wall boundaries with zero heat flux. The mixed thermal boundary conditions are used for the glazed façade surface. One of the most demanding aspects of heat transfer through the glazed façade surface is the evaluation of the convection heat transfer coefficient. More than thirty different correlations are found in the literature to determine the external heat transfer coefficient for buildings. Palyvos [19] provided a summary of these correlations and recommended using the following correlation to calculate the heat transfer coefficient (h_c) for windward surfaces:

$$h_c = 4V_w + 7.4 \qquad (2)$$

where V_w is the wind velocity. With zero wind velocity, an external heat transfer coefficient value of 7.4 W/m^2-K is used in this study. A solar transmittance of 0.36 and an absorptivity of 0.175 is used in this study as was used previously during the study of atrium building at Concordia University. The modeling of the glazed façade is simplified as a single glazed wall with an effective thermal conductivity of 0.0626 W/m.K and a total overall thickness of 24 mm. The radiation exchange between the façade and the sky is also taken into account. The sky temperature is calculated using the Mills' correlation [20] given as $T_{sky} = [\ \varepsilon_{sky} T_{out}^{\ 4}]^{1/4}$ where the emissivity of the sky, ε_{sky}, is calculated using the relation, $\varepsilon_{sky} = 0.727 + 0.006 T_{out}$. The heat sources are modeled as a no-slip wall boundary (2m x 2m) located in the centre of each floor. In all cases a heat source of 823W is assumed approximately equivalent to 4 sitting persons with desktop computers on each room floor and a heat source of 530W is assumed approximately equivalent to 7 resting persons on the atrium floor. A constant relative pressure of 0 Pa is used across the room inlets and the atrium outlets. An inlet turbulence intensity of 0.05 is applied at all the inlets as a boundary condition.

B. *Radiation Model*

To account for radiation, the radiation intensity transport equations (RTEs) are solved. Local radiation absorption by the fluid and at the boundaries links the RTEs with the energy equation. The wall glazing of the façade partially absorbs the radiation falling on it and transmits the remaining radiation which heats up the interior surfaces of the building. A solar calculator is used to determine the sun's location on the sky by inputting the time, date and the global location of the building. A solar calculator is also available in FLUENT© to calculate the beam direction and irradiation. The DTRM radiation model is found suitable to model the radiation for the present study. The main assumption followed in the DTRM model is that radiation leaving a surface element in a specific range of solid angles can be approximated by a single ray. It uses a ray-tracing algorithm to integrate radiant intensity along each ray and is a relatively simple model. Accuracy can be increased by increasing the number of rays to a wide range of optical thicknesses.

C. *Turbulence Model*

Based on the atrium height, a Rayleigh number greater than 1.0 x 10^9 for the building geometry indicates the onset of turbulence in the flow field. Consequently a turbulence model has to be employed in the CFD simulations. When the first-order fluid parameters are of main concern (e.g., mean

Proc. of the Intl. Conf. on Advances In Civil, Structural And Construction Engineering - CSCE 2014.

ISBN: 978-1-63248-020-0 doi: 10.15224/ 978-1-63248-020-0-103

temperature and flow rate) rather than turbulent fluctuation details, generally two equation eddy-viscosity turbulence models are found suitable for modeling internal flows. From past experience [7], the SST k-ω turbulence model has been found suitable for the present CFD simulations.

D. Model Validation

The results of the CFD model used in this work are validated against the previous work of Hussain and Oosthuizen [8-10] in which the airflow and temperature distributions were predicted in the atrium space of the Engineering building at Concordia University, Montreal, and an atrium building in Ottawa, Canada. The CFD results have also been compared with the experimental data available for the Concordia University Building. A close agreement is seen between the CFD predictions and experimental measurements demonstrating the capability of the CFD model to accurately predict the three-dimensional buoyancy-driven displacement ventilation flows in multi-storey spaces connected to a common atrium.

E. Mesh Generation

Using the commercial software GAMBIT©, a 3-d mesh with hexahedral/tetrahedral cells is created for the atrium building being studied. A finer mesh is used near the walls to facilitate better modeling of sharp gradients encountered near the walls. The mesh along the vertical (x-y) plane parallel to the façade glazing surface is shown in Figure 2. Three different mesh sizes are investigated: Mesh 1 (440,000 cells), Mesh 2 (834,000 cells shown in Figure 2) and Mesh 3 (1,275,000 cells). In all the three meshes, the cell density is made higher in the regions where larger velocity and temperature gradients are expected i.e., near the walls, ventilation openings and the areas potentially occupied by the thermal plume in order to capture the details of the airflow in these areas.

F. Solution Procedure and Mesh Independence

The numerical solution procedure adopted in the previous studies [7-10] has been utilized for the present CFD simulations as well. The pressure coupling is made using the SIMPLE algorithm. The body force weighted scheme is used to discretize pressure-velocity coupling. The second-order upwind scheme is used to discretize the momentum, the turbulent kinetic energy, the dissipation rate and the energy conservation equations. These are solved in a segregated manner and a converged solution is obtained when enthalpy and other flow variable residuals are less than 10^{-3}. The under relaxation factors used for pressure, density, momentum, turbulent kinetic energy, turbulent dissipation rate, turbulent viscosity, and energy are 0.3, 1.0, 0.2, 0.8, 0.8, 1.0 and 0.9 respectively to reach a converged solution. Mesh independence for the three mesh sizes is checked by comparing the values of the volume flow rates in the rooms on the left-hand side of the building. The results are summarized in Table III which shows that Mesh 2 with 834,000 cells is suitable to accurately predict volume flow rates, the velocity and the temperature distributions in the building. Approximately 10000 iterations are required to reach a converged solution.

TABLE III. VOLUME FLOW RATES ON DIFFERENT FLOORS FOR THE THREE MESH SIZES

Floors	Volume Flow Rate (m^3/s)		
	Mesh1	***Mesh2***	***Mesh3***
Ground Floor	0.45	0.46	0.46
First Floor	0.43	0.44	0.44
Second Floor	0.34	0.35	0.36

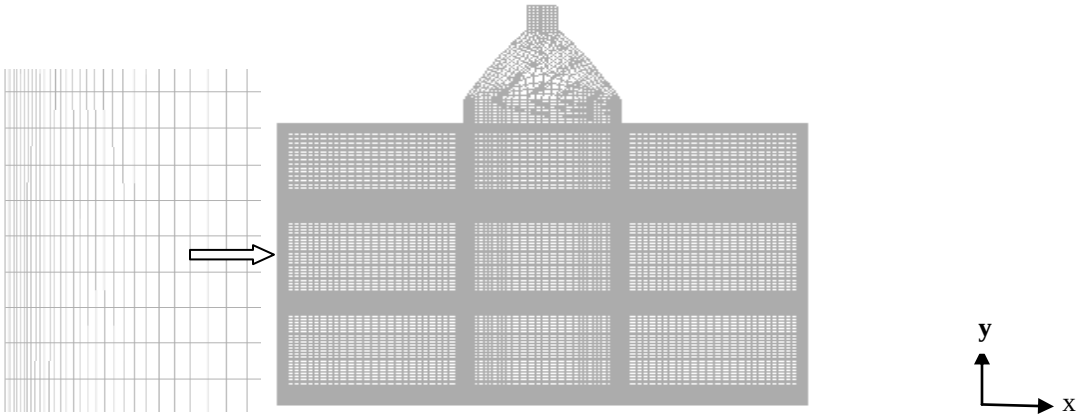

Figure 2: Computational mesh for CFD simulations (Mesh2) with near wall details.

Proc. of the Intl. Conf. on Advances In Civil, Structural And Construction Engineering - CSCE 2014.

ISBN: 978-1-63248-020-0 doi: 10.15224/ 978-1-63248-020-0-103

IV. Results

In practice, airflow inside the connected spaces is mixed by conduction, convection and radiation heat transfer effects. In this work, only interrelated conduction and radiation effects for the glazed façade wall have been considered while all the other walls are assumed to be adiabatic to match the assumptions of the mathematical models developed by Holford & Hunt [17]. As stated earlier, this model has been used to size the flow inlets and outlets on different floors. The proposed general ventilation concept involves fresh air being taken in from openings in the east and west facing walls, passing through the occupant spaces, and flowing out from upper openings between the rooms and the atrium. The air is finally exhausted from the atrium outlet at the top of the building. It is assumed that the driving force is the difference between the inside and outside temperatures of the building without considering the effects of external wind. Buoyancy-driven natural ventilation is more complex and difficult to model because of several parameters involved that are dependent and interdependent on the driving force of the ventilation. To cover all of these parameters is beyond the scope of the present study. In this work, factors such as climatic conditions, radiation intensity and the geographical location have been considered and will be discussed in detail to elucidate the performance of buoyancy-driven ventilation in the prototype building.

A. *Ventilation Volume Flow Rate and Temperature Distribution in the Building at Various Times of the Day and Locations*

Table IV(a) shows the results of volume flow rates of the buoyancy-driven ventilation on each floor at 9am, 1pm and 6 pm on 15 July 2012 in the rooms facing west while Table IV(b) shows these results for the rooms facing east and the atrium of the building for the three locations considered in this study. It can be noted that on the ground and first floors the ventilation flow rates are almost equal but on the second floor the flow rate is comparatively lower. This discrepancy can be attributed to the fact that buoyancy effects are higher on the ground and first floors as compared to the second floor. However, the design curves of Holford and Hunt use equal sizes of inlet openings for each floor to give approximately the same buoyancy-driven ventilation flow rate on every floor.

Figures 3a-3d show the contours of pressure, velocity, turbulence intensity, and temperature distribution at the mid-plane parallel to the facade of the building in Montreal at 1pm on 15th July 2012. Figure 3a shows the stack pressure effect resulting due to the pressure difference between the interior and exterior of the building. This difference is created naturally by density difference caused by warming of the air inside the building due to solar heat gain and the heat sources present in the building. This pressure difference drives the ventilation flow through the building by means of thermal stack effects. Figure 3b shows the velocity contours of buoyancy-driven ventilation airflow and indicates the influence of gravitational body forces on the velocity fields within the rooms and the atrium space. The natural convective flow over the hot surfaces can be clearly seen. Strong stack effect creates higher inflow on the lower floors than on the upper floors. Figure 3c presents the turbulence intensity contours at the mid-plane parallel to the facade of the building. The results show that turbulence intensity values are nearly uniform along the vents with a tendency of higher values near the outflow and in the regions where there is more mixing and circulation of the airflow within the building. Figure 3d shows the temperature distribution within the building. Higher air temperature stratification is observed near the ceilings of the rooms and near the outlet of the atrium. Lower temperature stratification near the floors is due to the strong convection.

B. *Effect of Solar Intensity and Geographical Location on the Buoyancy-driven Ventilation*

To determine the ability of the CFD model to predict the effect of solar intensity on the buoyancy-driven air flow at different times of the day, simulations are run at 9am, 1pm and 6pm. The outside boundary conditions such as outside air temperature and the positioning of the sun are adjusted for the selected times using the FLUENT solar calculator. Figures 4 and 5 show the results of (a) the pressure (Pa), (b) the velocity (m/s), (c) the turbulence intensity (%) and (d) the temperature (^{o}C) at the centre of the atrium and in the centre of the rooms respectively at 9am, 1pm and 6pm along the height of the building located in Montreal.

It can be seen that with the change in solar intensity and ambient temperature, the stack pressure developed inside the building varies and as a result it affects the volume flow rate, turbulence intensity and temperature distribution. With the increase of solar intensity, the volume flow rate increases at 1pm and then decreases at 6pm with the decrease in solar intensity. The effect of solar intensity also depends on the direction and location of glazing surfaces of the building. The effect of the geographical location on the buoyancy-driven ventilation flow rates is studied by considering the same building with the same orientation but located in different cities of Canada. Due to the different global location of each city, variations in solar loading existed in each case. The solar flux and the ambient temperature values summarized in Table II are used in the calculations. A comparison of (a) pressure (Pa), (b) velocity (m/s), (c) turbulence intensity (%) and (d) temperature (^{o}C) profiles in the centre of the atrium and rooms at 1 pm along the height of the building located in Saint John, Montreal and Vancouver are shown in Figures 6 and 7 respectively.

Proc. of the Intl. Conf. on Advances In Civil, Structural And Construction Engineering - CSCE 2014.

ISBN: 978-1-63248-020-0 doi: 10.15224/ 978-1-63248-020-0-103

TABLE IV(a). VOLUME FLOW RATES AT 9AM, 1PM AND 6 PM ON 15 JULY 2012 IN THE WEST FACING ROOMS OF THE BUILDING AT SAINT JOHN, MONTREAL AND VANCOUVER.

West facing rooms	Saint John Volume flow rate (m^3/s)			Montreal Volume flow rate (m^3/s)			Vancouver Volume flow rate (m^3/s)		
	9 am	1pm	6pm	9 am	1pm	6pm	9 am	1pm	6pm
First floor	0.45	0.41	0.34	0.45	0.39	0.34	0.44	0.46	0.35
Second floor	0.41	0.39	0.32	0.41	0.37	0.32	0.40	0.41	0.34
Third floor	0.29	0.31	0.28	0.27	0.29	0.28	0.28	0.30	0.30

TABLE IV(b). VOLUME FLOW RATES AT 9AM, 1PM AND 6 PM ON 15 JULY 2012 IN THE EAST FACING ROOMS AND ATRIUM OF THE BUILDING AT SAINT JOHN, MONTREAL AND VANCOUVER.

East facing rooms	Saint John Volume flow rate (m^3/s)			Montreal Volume flow rate (m^3/s)			Vancouver Volume flow rate (m^3/s)		
	9 am	1pm	6pm	9 am	1pm	6pm	9 am	1pm	6pm
Ground floor	0.47	0.40	0.34	0.47	0.38	0.34	0.45	0.44	0.35
First floor	0.43	0.37	0.33	0.43	0.36	0.33	0.42	0.41	0.34
second floor	0.32	0.28	0.28	0.34	0.28	0.25	0.33	0.28	0.27
Atrium	0.87	0.74	0.60	0.88	0.74	0.60	0.83	0.86	0.61

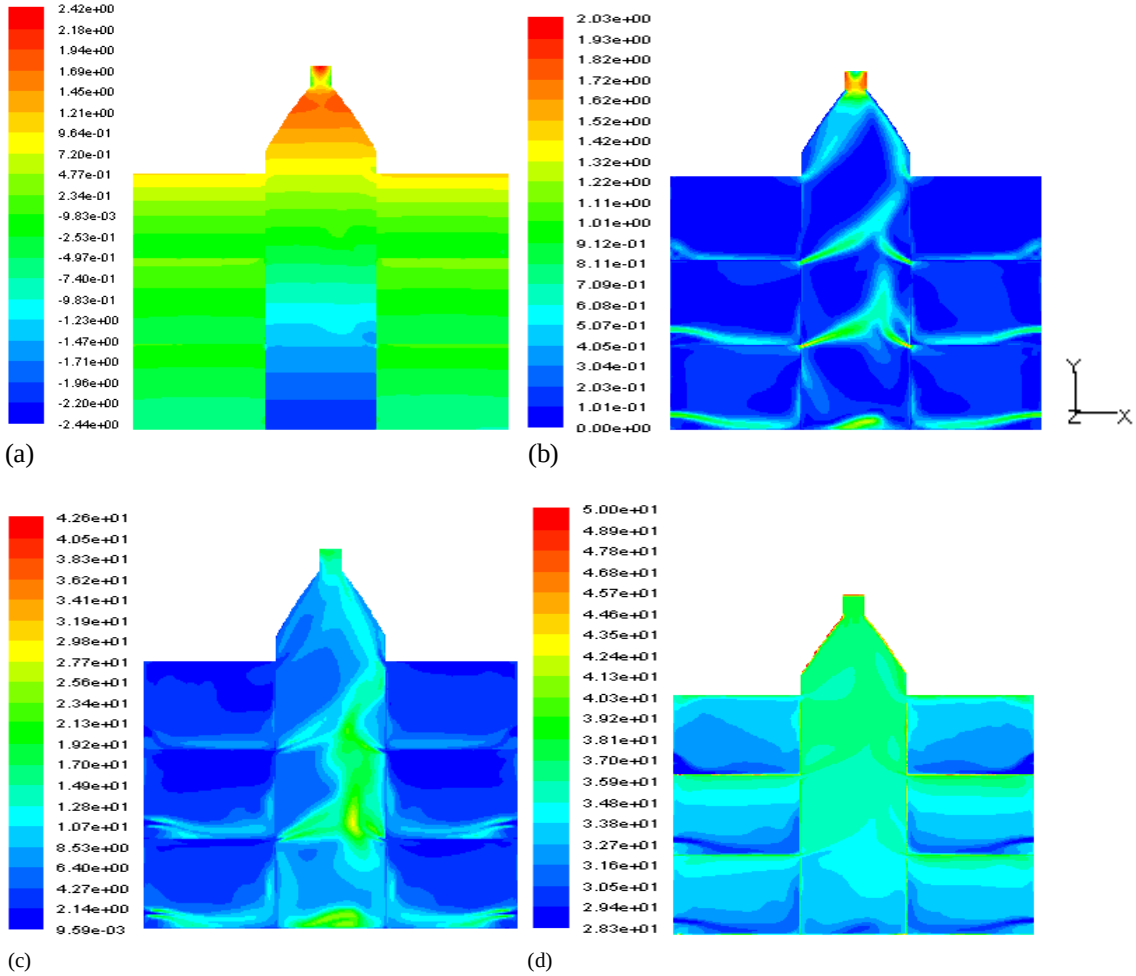

Figure 3: (a) Pressure [Pa], (b) velocity[m/s], (c) turbulence intensity[%], and (d) temperature [^{o}C] contours at mid-plane parallel to the facade of the building.

Proc. of the Intl. Conf. on Advances In Civil, Structural And Construction Engineering - CSCE 2014.

ISBN: 978-1-63248-020-0 doi: 10.15224/ 978-1-63248-020-0-103

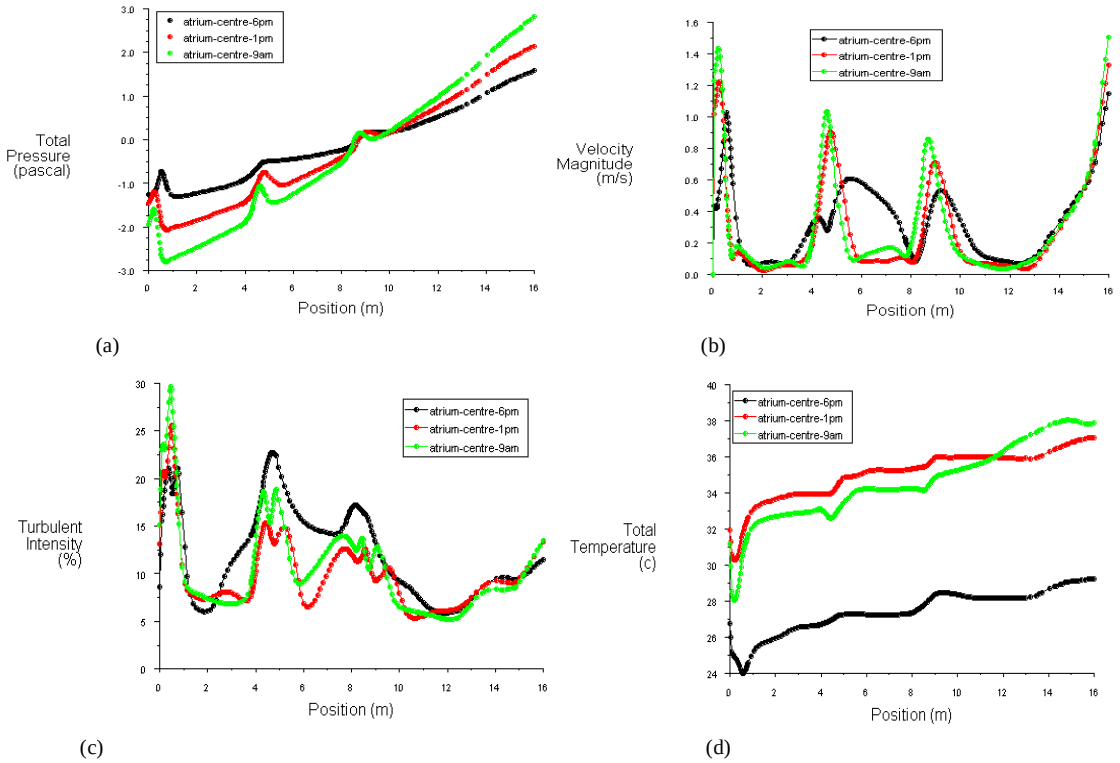

Figure 4: (a) Pressure (Pa), (b) velocity (m/s), (c) turbulence intensity (%) and (d) temperature (^{o}C) profiles in the centre of the atrium at 9am, 1pm and 6pm along the height of the building located in Montreal.

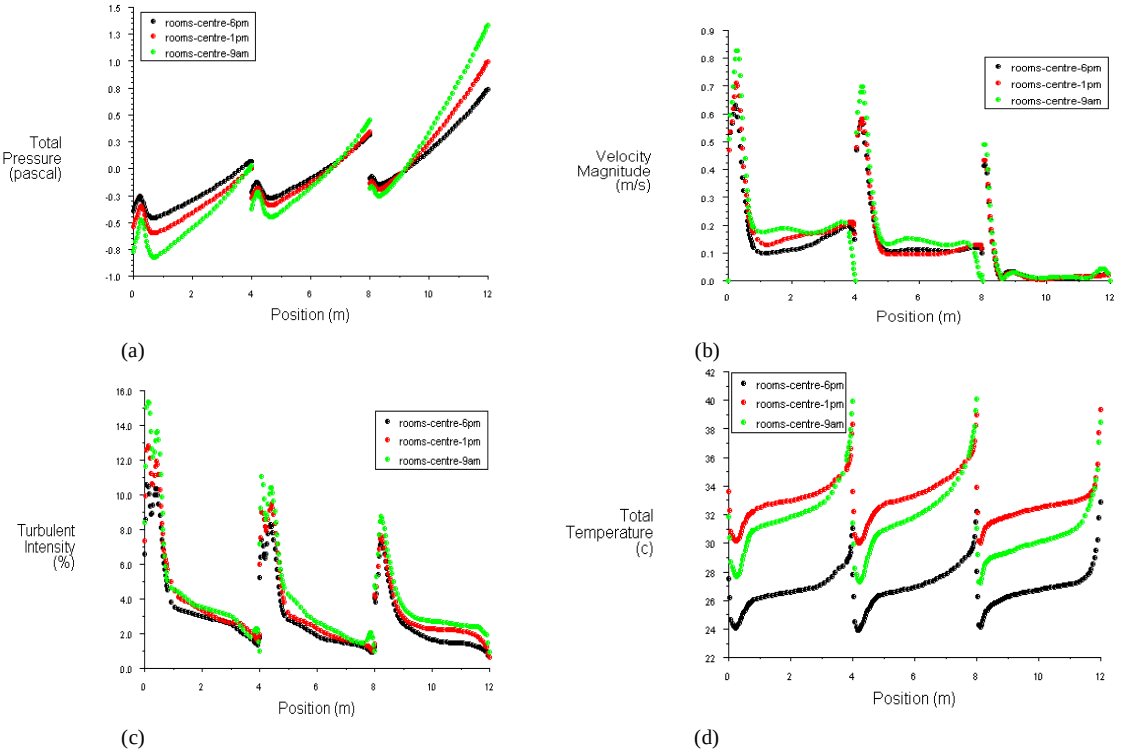

Figure 5: (a) Pressure (Pa), (b) velocity (m/s), (c) turbulence intensity (%) and (d) temperature (^{o}C) profiles in the centre of the rooms at 9am, 1pm and 6pm along the height of the building located in Montreal.

Proc. of the Intl. Conf. on Advances In Civil, Structural And Construction Engineering - CSCE 2014.

ISBN: 978-1-63248-020-0 doi: 10.15224/ 978-1-63248-020-0-103

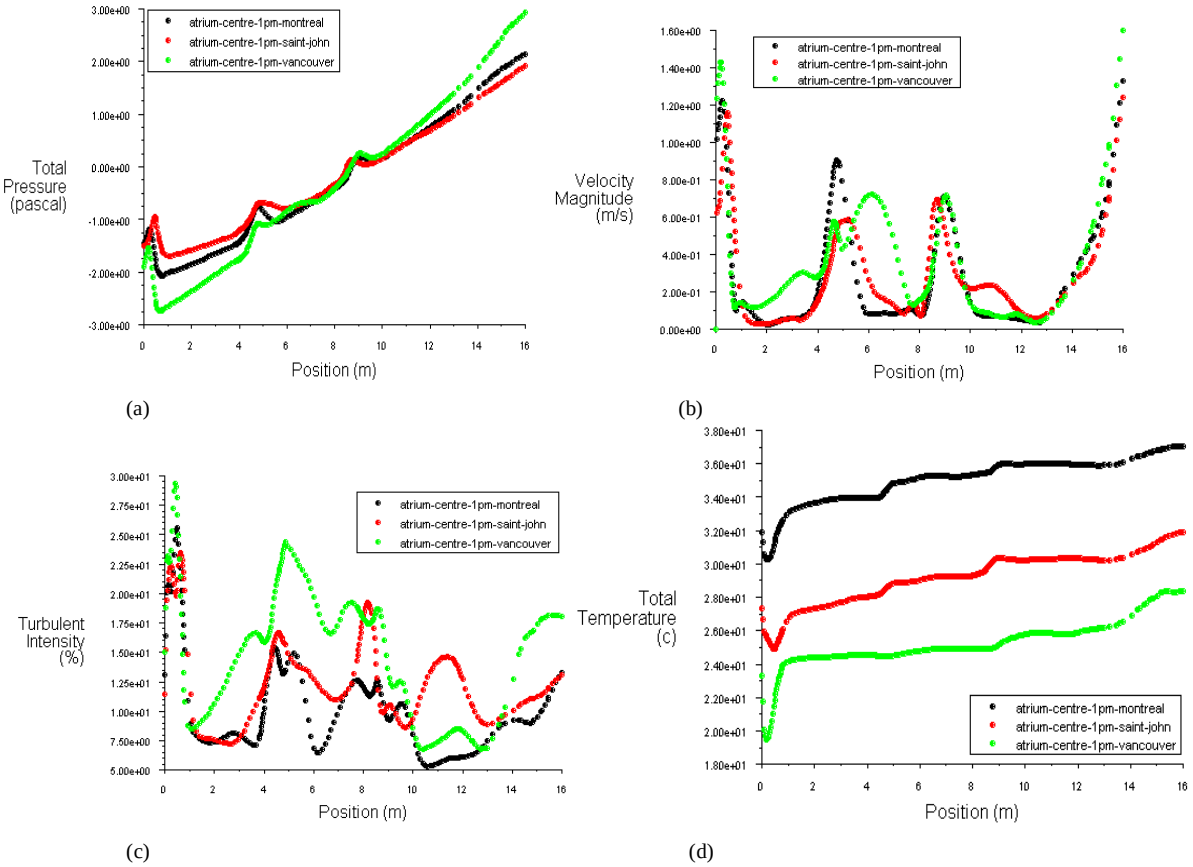

Figure 6: (a) Pressure (Pa), (b) velocity (m/s), (c) turbulence intensity (%) and (d) temperature (^{o}C) profiles in the centre of the atrium at 1pm along the height of the building located in Saint John, Montreal and Vancouver.

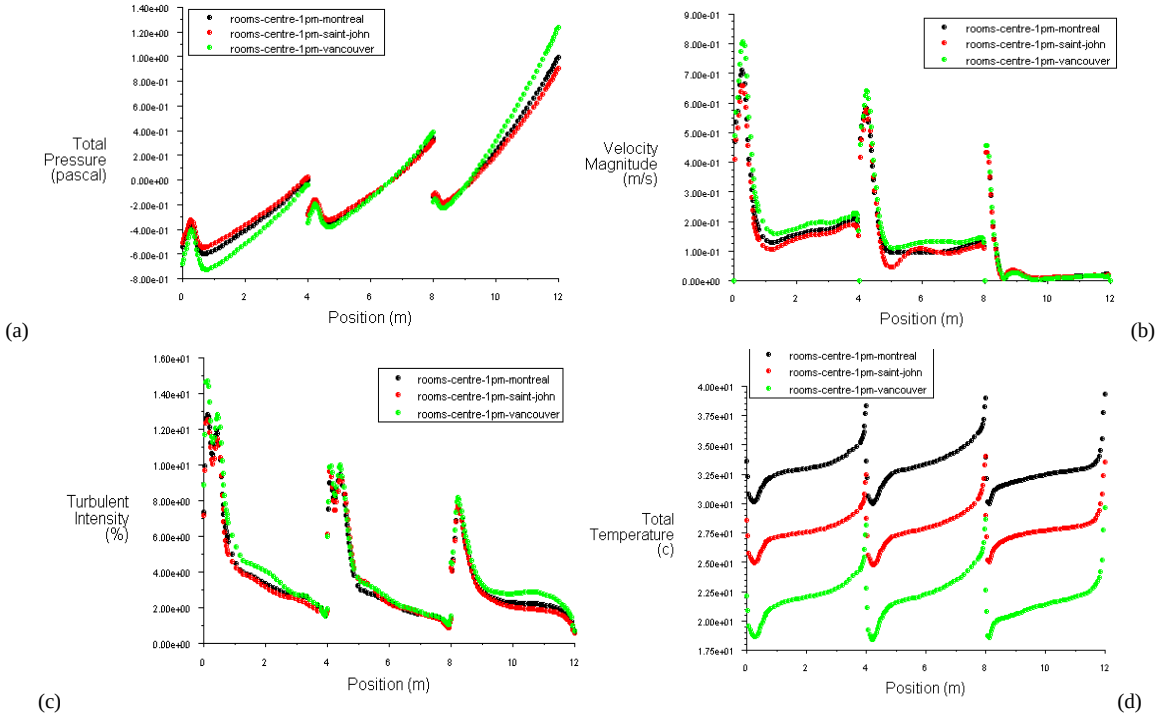

Figure7: (a) Pressure (Pa), (b) velocity (m/s), (c) turbulence intensity (%) and (d) temperature (^{o}C) profiles in the centre of the rooms at 1pm along the height of the building located in Saint John, Montreal and Vancouver.

Proc. of the Intl. Conf. on Advances In Civil, Structural And Construction Engineering - CSCE 2014.

ISBN: 978-1-63248-020-0 doi: 10.15224/ 978-1-63248-020-0-103

It can be seen from these figures that the solar heat flux in the cities considered varies and these variations directly affect the stack pressure, velocity, turbulence intensity and temperature distributions in the building.

v. Conclusions

In this study, a simple three-storey atrium building with a glazed roof is modeled and the results of buoyancy-driven natural ventilation induced by solar radiation and heat sources are presented using a validated CFD model. Steady-state CFD simulations of the buoyancy-driven natural ventilation airflow and temperature distributions in the building are carried out utilizing the SST k-ω turbulence model and the DTRM radiation model. The following main conclusions can be drawn from this study.

1. The design curves developed by Holford & Hunt are a useful tool in establishing the sizes of inlets and outlets in order to equalize ventilation flow rates on each floor of an atrium building.
2. The simulation results show that the solar intensity, ambient temperature and geographical location, all have a significant influence on the buoyancy-driven airflow rate and the temperature distribution inside the building.
3. In hot and humid weather such as in Vancouver, a building would require significant height to induce sufficient pressure gradient caused by temperature difference for efficient buoyancy-driven ventilation.
4. CFD techniques can be applied to real buildings to predict airflow parameters such as stratification depth, buoyancy of the upper layer and ventilation flow rate provided that the effective opening areas are accurately represented. For a comfortable indoor thermal environment, such techniques can be employed at the initial design stage of energy efficient atrium buildings.

Acknowledgment

This work was supported by Natural Sciences and Engineering Research Council Canada (NSERC)

References

[1] M. J. Cook, Y. Ji, G.R. Hunt, “CFD modeling of natural ventilation: combined wind and buoyancy forces,” Intl. J. of Ventilation, vol. 1, pp. 169-180, 2003.

[2] V. Anne, R. C. Francois, G. Gerard, “Thermal and ventilation modeling of large highly-glazed spaces,” Energy and Buildings, vol. 33, pp. 121-132, 2001.

[3] G. Guohui, “Simulation of buoyancy induced flow in open cavities for natural ventilation,” Energy and Buildings, vol. 38, pp. 410-420, 2003.

[4] J. Y. Tsou, “Strategy on applying computational fluid dynamics for building performance evaluation,” Automation in construction, vol. 10, pp. 327-335, 2001.

[5] P. H. Oosthuizen, M. Lightstone, “Numerical analysis of the flow and temperature distribution in an atrium,” Proc. of conf. on comp. methods for energy engineering and environment-ICCM3E, Sousse, Nov. 20-22, 2009.

[6] Y. Jiang, C. Allocca, C. Chen, “Validation of CFD simulations for natural ventilation,” Intl. J. of Ventilation, vol. 2, pp. 359-370, 2003.

[7] S. Hussain, P. H. Oosthuizen, A. Kalendar, “Evaluation of various turbulence models for the prediction of airflow and temperature distributions in atria,” Energy and Buildings, vol. 48, pp. 18-28, 2011.

[8] S. Hussain, P. H. Oosthuizen, “Numerical study of an atrium integrated with hybrid ventilation system,” Proc. of 23rd Canadian Cong. on Applied Mechanics, Vancouver, Canada, June 5-9, 2011.

[9] S. Hussain, P. H. Oosthuizen, “Numerical investigations of buoyancy-driven natural ventilation in a simple three-storey atrium building and its effect on thermal comfort conditions,” Applied Thermal Engineering, vol. 40, pp. 358-372, 2012.

[10] S. Hussain, P. H. Oosthuizen, “Validation of numerical modeling of conditions in an atrium space with a hybrid ventilation system,” Building and Environment, vol. 52, pp. 152-161, 2012.

[11] A. Atif, D. Claridge, “Atrium buildings, thermal performance and climatic factors,” ASHRAE Trans., vol. 101, pp. 454-460, 1995.

[12] T. Josef, H. Vitaly, T. Meir, “Airflow and heat flux through the vertical opening of buoyancy-induced naturally ventilated enclosures,” Energy and Buildings, vol. 40, pp. 637-646, 2008.

[13] A. Tahir, Y. Osman, “Investigating the potential use of natural ventilation in new building design,” Energy and Buildings, vol. 38, pp. 959-963, 2005.

[14] Y. Ji, M. J. Cook, V. Hanby, “CFD modeling of natural displacement ventilation in an enclosure connected to an atrium,” Building and Environment, vol. 42, pp. 1158-1172, 2007.

[15] M. J. Cook, K. L. Lomas, "Bouyancy-drriven displacement ventilation flows: evaluation of two eddy viscosity models for prediction," Building Services Engineering Research and Technology, vol. 19, pp. 15-21, 1998.

[16] C. Allocca, Q. Chen, L. R. Glicksman, "Design analysis of single-sided natural ventilation," Energy and Buildings, vol. 35, pp. 785-795, 2003.

[17] J. M. Holford, G. R. Hunt, “Fundamental atrium design for natural ventilation,” Building and Environment, vol. 38, pp. 409-426, 2003.

[18] http://www.climate.weather.gc.ca

[19] J. A. Polyvos, “A survey of wind convection coefficient correlation for building envelop systems modeling,” Applied Thermal Engineering, vol. 8, pp. 801-810, 2008.

[20] A. F. Mills, Heat Transfer, 2nd ed., Prentice Hall, NJ, 1999, pp. 570-572.